Interfacial Tension Measurements Using the Drop Profile Method

Eugene Wolfson
Senior Honors Thesis
Department of Physics
Brandeis University
2010

May 5, 2010

Abstract

An accurate, automatic method to measure interfacial tension of pendant drops is described. The physical setup and the software algorithm used are described and analyzed. Sources of error are investigated and simulation techniques used for characterizing the system are explored.

1 Theory

1.1 Interfacial Tension

Interfacial tension is the tension at an interface between two liquids. The study of interfacial tension is important in the phase chip where it is used "to sequester a large series of protein drops into individual compartments." The protein drops consist of a protein solution in an aqueous phase, surrounded by a buffer fluid. "The two fluids must be matched such that the interfacial tension between the aqueous protein phase and the continuous phase is great enough to promote the formation of individual drops, but not so great that the drops have a tendency to re-merge if they come back into contact with one another... The protein adsorption behavior at the interface between the continuous phase and the aqueous phase. If a surfactant is used to modify the interfacial tension between the two phases, it may have additional effects on the behavior of the protein suspended within the drop... By monitoring the time-evolution of the drop's surface tension, conclusions can be drawn about the rate and stability of protein adsorption at the interface. Establishing that protein concentrations are stable under controlled circumstances would add to the rigor and robust function of the phase chip."[5] We can use pendant drop profile method to measure the interfacial tension between aqueous protein drops in a buffer solution, such as silicone oil, optionally with surfactants.

It was determined by Young-Laplace that, in a system where a drop of one liquid is suspended from a circular capillary into the phase of another liquid, the surface of the formed drop can be used to extract the interfacial tension of the system. The system is referred to as a pendant drop. This method benefits from being static: "once the surface is formed, it is not subjected to any changes due to outside influence prior to or during the measurement. It... permits an accurate study of changes in surface composition with time, a phenomenon of predominant importance in the study of various colloidal systems."[1]We begin this paper by looking at the equations used to describe the profile of a pendant drop. We continue by describing the hardware and software of a prototype of a tensiometer developed in house. We end by characterizing the accuracy of the tensiometer.

1.2 Young-Laplace Equations

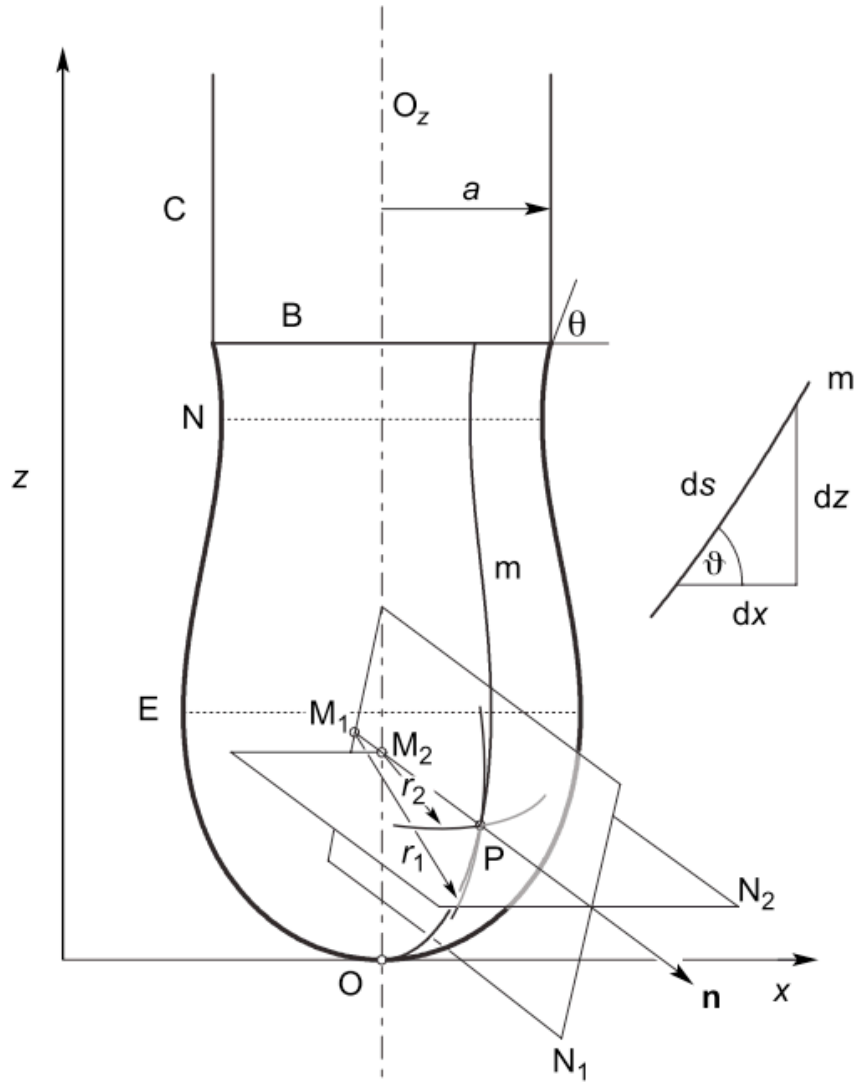

Figure 1: "The surface of a pendant drop hanging on the axisymmetric capillary C of radius a in the cartesian coordinate system x, y, z with origin O. The basis B of the drop is at the end of the capillary. For a given point P on the drop surface three mutually orthogonal planes crossing at P can be plotted: the tangential plane and two planes N_1 and N_2. The plane N_1, containing the symmetry axis O_z, cuts the surface of the drop in the meridian m. M_1 and M_2 are the centers of the circles of curvature with radii r_1 and r_2, respectively. **n** is the normal to the surface. ϑ is the inclination angle or the angle between the tangential plane and the horizontal plane z = 0. The contact angle of the drop at the basis of the capillary is θ. The inset [triangle] shows a small portion of the meridian m to define infinite small increments of the meridian length s and the corresponding coordinates x and y." Both graphic and caption are from Meister.[2]

Most of the theoretical derivation follows that of Meister. Other than slight changes in notation, refer to Figure 1 as a graphical aid.

The relationship between the shape of liquid drops and the pressure difference along the drop interface is governed by the equations of Young and Laplace, expressed as

$$\Delta p = \gamma \left(\frac{1}{r_1} + \frac{1}{r_2} \right) \tag{1}$$

Where Δp is the difference in pressure on the concave side of a curved liquid surface to the pressure on the opposite side, the proportionality factor γ is the interfacial tension of the drop, and r_1, r_2 are the principal radii of curvature to a point P on the drop surface.

Being axisymmetric about O_z, the drop is a figure of revolution about the vertical axis through the origin. This means that we only need information about a single slice through the O_z axis to discuss the shape of the drop. This slice is referred to as the drop profile. The profile actually contains twice as much information as we need. Specifically, only half the meridian from the apex to the basis is required. This allows us to easily relate the final form of the Young-Laplace equations, below, directly to an extracted drop profile.

The optical setup allows us to image a silhouette of the drop, the outer profile of which can be described by either Cartesian coordinates x, z or the meridian pathlength s and a local inclination angle ϑ to the outside of the profile. This silhouette's outer edge is the meridian along the x-z axis and s is the pathlength along that meridian. At a point along this edge, we define the vertical curvature as

$$r_1 = \frac{ds}{d\vartheta} \tag{2}$$

and the lateral curvature as

$$r_2 = \frac{x}{\sin \vartheta} \tag{3}$$

Substituting equations 2 and 3, for r_1 and r_2, equation 1 becomes

$$\Delta p = \gamma \left(\frac{d\vartheta}{ds} + \frac{\sin \vartheta}{x} \right) \tag{4}$$

Since the drop is a figure of revolution through the apex, we know that both radii of curvature must be the same at the apex. We denote the radius of curvature at the apex, where $r_1 = r_2$, as b. Thus, the pressure differential at the apex is $\Delta p_{apex} = \gamma \left(\frac{1}{b} + \frac{1}{b} \right) = \frac{2\gamma}{b}$. If $\Delta\rho$, the difference in density between the drop and the surrounding phase, is greater than zero, then we know that Δp_{apex} is the point of maximal pressure difference. This is the case for a hanging pendant drop. If, on the other hand, $\Delta\rho < 0$ the analysis is the same, but signs are reversed. In this paper, we rotate inverted pendant drops and treat them as hanging pendant drops for the purpose of determining interfacial tension.

We know from hydrostatics that at any vertical point in the drop, the pressure difference at that point varies linearly with respect to the height from the apex. Since Δp_{apex} is the point of maximal pressure difference,

$$\Delta p = \Delta p_{apex} - \Delta\rho g z = \frac{2\gamma}{b} - \Delta\rho g z \tag{5}$$

where $\Delta\rho = \rho_{drop} - \rho_{phase}$ and ρ is the density of the subscripted material. Note that $\rho_{drop} > \rho_{phase}$ for a pendant drop hanging in the direction of gravity. Otherwise, the drop's density is less than its surrounding phase and it will attempt to float through its surrounding medium. In this case, the base of the drop must be inverted.

We can combine equations (4) and (5) to get, step by step:

$$\gamma\left(\frac{d\vartheta}{ds} + \frac{\sin\vartheta}{x}\right) = \frac{2\gamma}{b} - \Delta\rho g z$$

$$\left(\frac{d\vartheta}{ds} + \frac{\sin\vartheta}{x}\right) = \frac{2}{b} - \frac{\Delta\rho g z}{\gamma}$$

$$\frac{d\vartheta}{ds} = \frac{2}{b} - \frac{\Delta\rho g z}{\gamma} - \frac{\sin\vartheta}{x}$$

$$\frac{d\vartheta}{ds} = \frac{2}{b} - \frac{z}{a^2} - \frac{\sin\vartheta}{x} \tag{6}$$

where $a = \sqrt{\frac{\gamma}{\Delta\rho g}}$, in meters, is the capillary constant and b the radius of curvature at the apex, in meters, is the shape parameter.

Notice that at the apex, $s = x = z = 0$, leaving equation 6 undefined. For this initial case, we refer to the definition of curvature, $\kappa \equiv (d\vartheta)/(ds)$ where ϑ is the inclination angle and s is the pathlength. Noting that the radius of curvature is the inverse of curvature, and that the radius of curvature at the apex is b, we have an addendum that

$$\begin{cases} \frac{d\vartheta}{ds} = \frac{2}{b} - \frac{z}{a^2} - \frac{\sin\vartheta}{x} & s > 0 \\ \frac{d\vartheta}{ds} = \frac{1}{b} & s = 0 \end{cases} \tag{7}$$

Remember, as illustrated in Figure 1, that ds is an infinitesimal step along the drop's profile and that we define dx and dz as the legs of a right triangle with ds acting as the hypotenuse. $d\vartheta$ is the angle between the curve and the horizontal - the angle between dx and ds. From here, it is a trivial trigonometric statement that

$$\frac{dx}{ds} = \cos\vartheta \tag{8}$$

$$\frac{dz}{ds} = \sin\vartheta \tag{9}$$

Equation 7 has no known analytical solution, but we can solve it numerically to get the coordinates of a drop between the apex and the basis. As a drop increases in volume, the pathlength of its meridian and its shape does too. Eventually a drop is said to reach a critical volume, where any increase in its volume causes the drop to separate from the capillary. For a given capillary constant a, a critical drop has a unique critical shape parameter b for each capillary of radius r_{cap}. If the curve $x(s)$ reaches its second point of inflection, then, the drop is at a critical volume. The pathlength at that point is denoted s_c, the critical pathlength, and any points on the curve past s_c do not represent physical drops. On the other hand, all subcurves with pathlength $s_{max} \leq s_c$ represent physical drops with a capillary radius $r_{cap} = x(s_{max})$. Of course, s_c is different for each combination of parameters. In conclusion, we can solve the Young-Laplace equation for a given b and a and r_{cap}, those drops with a capillary radius of r_{cap} represent pendant drops of shape parameter b and capillary constant a hanging from a capillary of radius r_{cap}.

1.3 Estimation methods

In practice, fitting methods are generally only as good as their initial guess. The equations of Young-Laplace are no exception. In order to avoid getting stuck in a local minima, we need to provide initial guesses close to the exact values. These values can be provided manually by a user, but there are also other, automatable, ways of estimating the parameters.

1.3.1 Selected Plane Method:

A classic method of determining interfacial tension from pendant drop profiles is called the selected plane method. Although the selected plane method is not as accurate as fitting, we can use it to quickly estimate the capillary constant a. We follow the derivation of Andreas, with some adaptations of notation.[1] The basic presime of the method is to relate the size of the drop S to a table of values H, where H depends on the ratio of the capillary constant a and the equatorial diameter of the drop d_e, and S depends on the ratio of d_e and a selected plane diameter d_s. d_e is the maximal width of the drop at the plane labeled E, and d_s is the width of the drop at the height d_e from the apex. Specifically,

$$S = \frac{d_s}{d_e} \tag{10}$$

$$H = d_e^2/a^2 = \frac{g\Delta\rho(d_e)^2}{\gamma}$$

$$a = \sqrt{\frac{d_e^2}{H}} \tag{11}$$

Since a drop's shape can be specified by b, we can create a table relating S to H. To do this, we solve a series of Young-Laplace equations by varying b and keeping all other parameters constant. We use the resulting drop profiles to measure d_s, d_e. Using the values of a, d_s, and d_e and equations 10 and 11, we can write a table relating S to H^{-1}. If given a drop profile of known $\Delta\rho g$, we can measure d_e and d_s to find S. From there it is a matter of looking up the value of H^{-1} from the table and plugging it into Equation 11.

In practice, this method suffers from a limited accuracy. The position of each point of a drop is not absolute. Vibration, and finite camera resolution means that each drop profile coordinate is stochastic to a small degree. Thus, the acuracy of the selected plane method, which considers only two points to define the shape of the drop, is limited by the accuracy to which these two points can be determined. The benefit of using the whole drop profile via fitting is that the interfacial tension error diminishes with an increase in the number of points considered for the drop profile due to the law of large numbers. [3] [1]

The other consideration is the precision of the S vs. H^{-1} table. The table can be as accurate as the integration of the Young-Laplace equations, but eventually lookup time will become an issue; however, with S determined to just three significant digits, the initial guesses are good enough that simulated drops are accurate to within 1% after fitting. Since physical drops are constrained to $S \in (0, 1)$, that means the table need only hold 1,000 values. Most of these values will never be encountered with real drop systems, as S is rarely under 0.5.

There is also the limitation that for some drop shapes d_s is undefined. This can happen when the equator is wider than the height of the drop, or the equator, of width d_e is located higher than a distance d_e from the apex. These drops are of type I as defined by Meister and Latychevskaia.

1.3.2 Oscullating circle

In order to provide a quick estimate of the shape parameter b, we need to estimate the radius of curvature at the apex of the drop. One approach is to fit an oscullating circle on the interior of the drop profile, tangent to the apex. "The osculating circle of a curve C at a given point P is the circle that has the same tangent as C at point P as well as the same curvature. Just as the tangent line is the line best approximating a curve at a point P, the osculating circle is the best circle that approximates the curve at P... Given a plane curve with parametric equations $f(t)$ and $g(t)$ and parameterized by a variable t, the radius of the osculating circle is simply the radius of curvature" [4]

If our optics were perfect, we could extract the exact b using this method; however, information about the apex is limited by the apex's small size. The resolution of our camera limits how accurately we can specify the apex, so we depend on the locality of curvature at the apex. If we assume that the change in curvature near the apex is small, then we can use a small section of the curve near the apex to fit an oscullating circle. The drop profile is a plane curve with parametric equations $z = f(x)$. We fit an osculating circle at the apex $z = x = 0$ following the derivation adapted from Johan Claeys:[6]

Take a small enough portion of the curve near the apex such that it can be accurately fit to a polynomial equation. We consider what constitutes a small enough portion in section 3.1.5. From the equation of a circle we have $(x - x_c)^2 + (z - z_c)^2 - b^2 = 0$, with the three parameters x_c, z_c, and b being the center and radius of the oscullating circle. Using implicit differentiation for z we arrive at z', z'':

$$\begin{cases} (x - x_c)^2 + (z - z_c)^2 - b^2 = 0 \\ (x - x_c) + (z - z_c)z' = 0 \\ 1 + (z')^2 + (z - z_c)z'' = 0 \end{cases} \tag{12}$$

[1] In Table 2 of Song's paper, there is a detailed study on the accuracy of determining γ with simulated water drops of varying edge quality and point quantity.

Since $z = f(x)$, at the apex we denote the values of z, z', and z'' as $f(x_0)$, $f'(x_0)$, and $f''(x_0)$, respectively, with x_0 the value of x at the apex. This notation is more explicit for fitting. At the apex, equation 12 becomes

$$\begin{cases} (x_0 - x_c)^2 + (f(x_0) - z_c)^2 - b^2 = 0 \\ (x_0 - x_c) + (f(x_0) - z_c) f'(x_0) = 0 \\ 1 + (f'(x_0))^2 + (f(x_0) - z_c) f'' = 0 \end{cases}$$

which we use to solve for the three parameters x_c, z_c, and b:

$$x_c = x_0 - f'(x_0) \frac{1 + f'(x_0)^2}{f''(x_0)} \tag{13}$$

$$z_c = f(x_0) + \frac{1 + f'(x_0)^2}{f''(x_0)} \tag{14}$$

$$b = \left| \frac{\left(1 + f'(x_0)^2\right)^{3/2}}{f''(x_0)} \right| \tag{15}$$

Note that x_c should be zero since x coordinate of the apex, x_0, is defined to be zero.

2 Setup

2.1 Optics

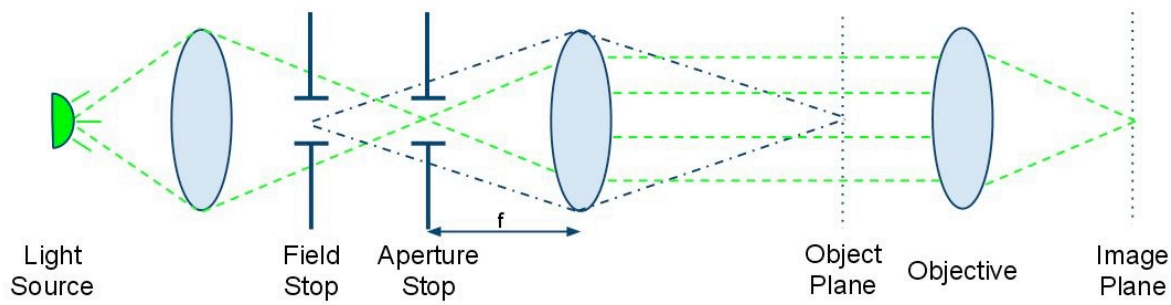

Figure 2: Optical Diagram. The green dashed line represents the path of light from the light source to the image plane. The dashed-and-dotted black line represents a light path from the object plane and focused where the field stop is positioned. f is the focal length of the lens immediately to the right of the aperture stop.

2.1.1 Koehler Illumination

In order to get uniform illumination we set up Koehler illumination, as illustrated in figure 2.

The light source is focused one focal length f from a lens of focal length f. Light on the opposite side of the lens comes out parallel by the Thin Lens Equation $\frac{1}{focal\,length} = \frac{1}{object\,distance} + \frac{1}{image\,distance}$, where $object\,distance = focal\,length$, so $image\,distance$ is infinite.

The aperture diaphragm, also called aperture stop, is used to control the intensity of the light in the object plane. The aperture stop is placed one focal length away from the lens. The field diaphragm, also called field stop, is used to control the field of view. If the setup is as in Figure 2, then the diaphragms control the intensity and field of view independently of the other diaphragm.

We can check that we are in focus by closing the field stop so that it is almost shut and observing that its edges are in sharp focus. We can use the field stop to control the size of the illumanition circle and to set the height of components along the optical path. With the field stop almost closed, the small circle of light on the image plane represents what should be the center of the image.

The optical setup needs to project a drop of some size onto a CCD of another size. Drops with high surface tension can become very large before detaching from the needle. For example, in the current setup, water

drops in a PDMS oil system are larger than the CCD, so we need to demagnify the image. Some drops are so large that the size of the illuminated area becomes a concern. The illuminated spot must be larger than the drop size.

More detailed instructions on setting up Koehler illumination are in section 4.1.

2.1.2 Index Matching the Cuvette

Drops in a fluid phase require a container to hold the fluid. We use a square, disposable spectrophotometer cuvettes with a 1 cm^2 cross-sectional area because they are transparent, cheap, and small enough to limit the quantity of material used, but large enough to house all but the largest drops from standard capillaries with a needle gauge between 15 and 23. Despite these benefits, the walls of the cuvette have a different index of refraction from the air outside the cuvette and so the defects on the cuvette have a high level of contrast to the background illumination. We can reduce this contrast by surrounding the outside of the cuvette with an index matching fluid, such as water. Since the inside of the cuvette is full of a fluid already, we effectively index match the walls of the cuvette. Therefore, only the drop and the tip of the needle have a high level of contrast to the background.

2.2 Syringe Controller

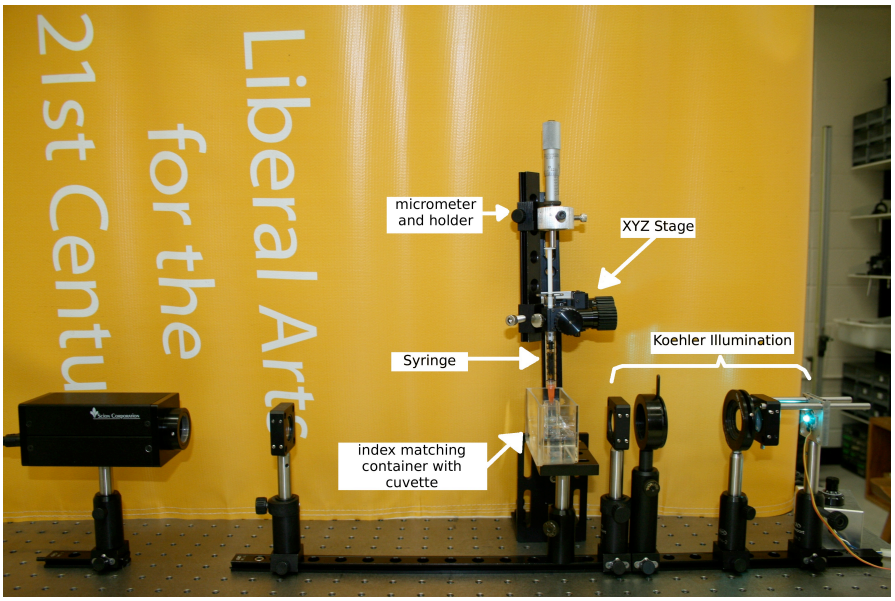

(A)

(B)

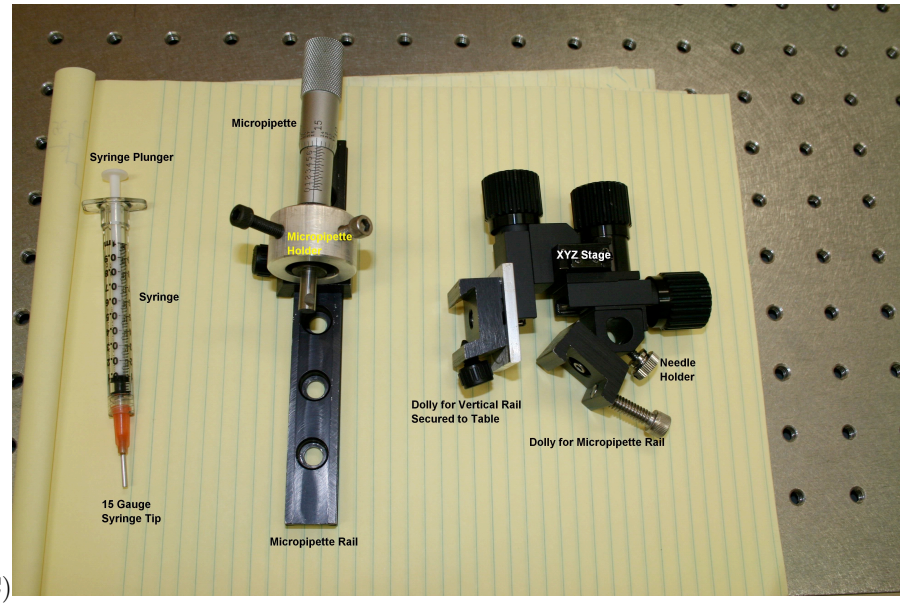

(C)

Figure 3: A) Photograph of the whole setup with Koehler Illumination set up to the right of the syringe. The syringe marks the object plane. In this image, the index matching container is full of water with the cuvette visible inside, below the syringe. B) Close-up of the object plane. No index matching container is used so that the cuvette is easy to seer. C) Close-up of the individual components of the syringe controller, left-to-right: a sample syringe with a 15 gauge tip, micrometer in holder on rail, and XYZ stage. The distance between each row on the legal pad is 0.5 cm.

In the experiments, a syringe tip acts as a circular capillary to dispense a pendant drop into some fluid (be it liquid or air). In order to place a syringe in the object plane, we place it into a needle holder suspended above the object plane. The needle holder is attached to an XYZ stage held by a dolly on a vertical rail secured to a vibration-resistant table, as seen in Figure 3B. Also seen from 3B, is a micrometer resting above the syringe's plunger. The micrometer and syringe are held in place relative to one another by a rail secured to a dolly adjacent to the needle holder on the XYZ stage.

Once the three components, shown separately in figure 3C, are put together they can be slid up and down the rail secured to the table, without changing their relative positions. if the experimenter needs to access the area near the intersection of the object plane and the optical path, the focus will not be upset: the dolly holding the XYZ stage to the vertical rail secured to the table is slid up and only the Z position needs to be set to regain focus. To achieve focus initially, we use the XYZ stage help manuever the needle into the object plane.

The micrometer is used to push the syringe plunger in a controllable, and repeatable way. Its position relative to the needle holder can be changed by sliding the micrometer dolly along the rail secured to the needle holder's dolly - this is useful if the micrometer is fully extended and syringe is still full. See Section 4.2 for more instructions.

Drop tilt has been found to be a large source of error.[3]This source of error comes from the tilt of the syringe. The needle holder should orient the needle tip toward $\vec{g}$. When the syringe is passed through the needle holder, a thumb screw on the side of the needle holder needs to be tightened to pin the syringe to the needle holder. In general, the syringe will end up pinched at a small angle to the vertical, meaning that the tip is also at a small angle. Pinning the syringe keeps it from rattling about as the micrometer pushes down on the syringe plunger; however, since the micrometer and needle holder are secured to the same rail, any vibrations caused by spinning the micrometer are transferred through the rail and into the needle, causing the drop at its tip to vibrate.

Another source of tilt comes from an imperfectly aligned camera. If our camera is at a non-zero angle to $\vec{g}$, then all images will have a systematic tilt to them as well. A bubble measure on top of the camera can tell us to about a degree of accuracy, how tilted the camera is. We can also take a series of images of a plumb bob and the average angle of the plumb bob should tell us how tilted the camera is. All images taken by the camera can then be rotated to reverse the tilt from the camera.

3 Software

A Matlab program was developed to measure the interfacial tension of pendant or inverted pendant drops. It should be available online at Matlab Central File Exchange.

3.1 Tensiometer Software

3.1.1 GUI

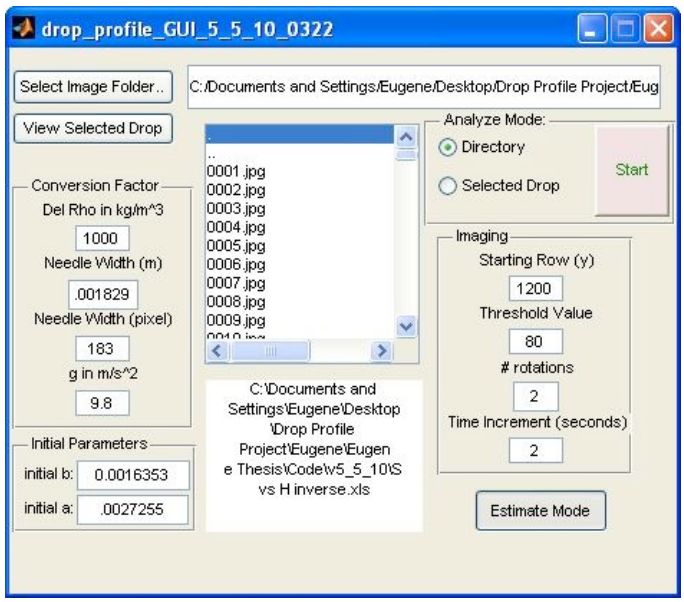

Figure 4: GUI Interface. See section 4.3 for a Description of the inputs.

A GUI, shown in figure 4, is used to input the experiment's parameters. The GUI is responsible for specifiying which images to measure and saving those measurements to disk. Along with sending images to the back end, described below, the GUI provides the back end of the program with the parameters it requires. These include the conversion factor, scaling factor, starting row, S vs. H^{-1} table or initial guesses for b and a, and other imaging parameters. The conversion factor
$conv = (\Delta\rho \text{ in kg/m}^3) * (g \text{ in m/s}^2)$ in units of $(\text{kg/m}^3)(\text{m/s}^2) = \text{kg} * \text{s}^{-2} * \text{m}^{-2}$.
Scaling factor = (Needle Width in m)/(Needle Width in Pixels) is used to scale extracted curves from pixel units to meters before fitting them to theoretical curves expressed in meters. The starting row is the first row of the image that is scanned in the edge extraction algorithm. Although this row could be found automatically through image processing, in general, a series of images in an experiment should have a constant starting row, so it is easier to specify one starting row for the whole experiment. The S vs. H^{-1} table used for estimating the capillary constant a as desribed in Section 1.3.1 is loaded only if estimation mode is on. If it is not, the GUI is expected to provide initial guesses for the shape parameter b and the capillary constant a.

Each image sent to the back end which is, loosely, the following four steps:

1. Imaging (Section 3.1.2)
2. Drop Edge Extraction (Section 3.1.3)
3. Choosing initial parameters b, and a through estimation (Section 1.3) or directly from by GUI
4. Calculating interfacial tension by fitting the Young-Laplace equations (Section 1.2 Equation 7)
5. Return information about drop.

When the back end returns a set of information it calculated about the drop the GUI is responsible for saving that data to disk, along with the settings that the user input.

3.1.2 Imaging

The imaging algorithm follows. An image is loaded from a filepath given by the GUI, its pixels transformed to normalized grayscale levels, and rotated into an inverted hanging drop. If the file can't be found, this image is skipped and a message is displayed to the user. If the image is successfully loaded into Matlab, it is converted into gray scale and then the average pixel value, $<$ pixel value $>$, of the image is normalized to 128. To achieve this the image is scaled by 128/ $<$pixel value$>_{original}$. Setting the average pixel value to 128, makes the absolute lighting conditions less important for thresholding the drop. As long as there is high contrast between drop and its background, the same threshold value can be set. The user doesn't need to consider the absolute value when deciding on a threshold. After setting the greyscale, the whole image is rotated so that the tip of the needle is at the bottom of the image with the drop apex above the needle tip. The rotation is achieved through a series of 90° counterclockwise rotations. The number of rotations is specified by the user through the GUI. By demanding that all drops are rotated to inverted hanging arrangement before extracting their edge, we reduce the complexity of the edge extraction algorithm, leaving it up to the user to specify the initial alignment of the drop through the number of rotations required to rotate the drop to inverted hanging arrangement. At this point the drop is ready for edge extraction.

3.1.3 Edge Extraction Algorithm

The edge extraction algorithm follows. Rows containing the drop are scanned from left to right to identify pixels below the threshold, specified by the GUI. At each scanned row, the first and last pixels below the threshold define the left and right edges, respectively, of the drop at that row. The first row scanned is the starting row. Each row above the starting row is scanned sequentially. The last row scanned is determined when we encounter a row with no pixels below the given threshold. At this point, the last row is set to the row immediately preceding the row with no edges found. If only one pixel is found at any row, the left and right edges at that row are equivalent. If any of the edges of the drop are detected at the boundary of the drop, the drop is invalid. If not enough rows contain an edge to extract meaningful information, the drop is also invalid. If a drop is marked as invalid, a message is displayed to the user that its edge was not found and this image is skipped.
Notice that this method we have two edges, and they are not necessarily equal about the vertical axis through apex - defined as the midpoint between left and right drop coordinates at the top most row of the drop; however, the theory demands that the drop be axisymmetric. Due to various sources of error, our drop may violate this symmetry. Nonetheless, we require axisymmetry to use equation 7. Specifically, we need a plane curve starting from the drop apex and ending at the drop basis. We have a few options. We may

try to correct some sources of error (such as tilt, and non smoothness of the drop edge), until our drop is axisymmetric - then we could use either of the edges. While it is impossible to perfectly correct the sources of error, it is still a good idea to try to reduced them as much as possible. Once we have massaged the drops, we still need to choose an edge. We could definitely choose either side of the drop, but it has been shown that we can increase the accuracy of the method further by choosing the mean edge.[3] Combine both edges by the following transformations:

Define the apex as the mean of both drops. Rotate and shift each edge so that both edges are in the first quadrant, with the apex at the origin. Now, we choose an edge to use with equation 7 by taking a point-by-point mean of both edges. This has been shown by Song to remove some of the error associated with tilt and smooth the drop profile. Finally, our profile is one curve with pixel coordinates. Since equation 7 is in units of meters, we should scale the profile from pixels to meters using the scaling factor Scaling factor = (Needle Width in m)/(Needle Width in Pixels). Now the profile is ready to be fitted to the Young-Laplace equations.

3.1.4 Estimating Parameters

For fitting, we need to have an initial guess, because a fitting method is only as powerful as its initial guess. The program allows for two methods of providing the fitting algorithm with an initial guess: an initial guess may be entered manually through the GUI, or it may be provided automatically through a pair of estimation methods described in Section 1.3. In this section we only have a few comments about the implimentation.

For the selected plane method, drops with values of S not within the table are constrained to the closest S value available in the table. As a result, drops with S outside the range of the table are set with values of H^{-1}, potentially far from the actual value. Erronious estimates can be reduced by improving the accuracy and range of the S vs. H^{-1} table as described in Section 1.3.1. If d_e is more than drop height, then d_s is unspecified for a drop, but the current implementation sets $d_s = d_{basis}$.

For the oscullating circle method, only 15 points starting from the apex of the circle are used - this number was determined to be sufficient by trial and error on a range of both simulated and real drop shapes. Given the current imaging setup and the resolution of the camera, 15 points is close enough to the apex that the curvature stays constant to degree of accuracy needed for estimating an initial value. If the drop has less than 15 points, which is possible for very small drops or a large demagnification, then all of the drop profile is used to fit an oscullating circle to the apex of the drop.

Note that in the current implementation, a mirror view of the drop profile is appended to act as a left side of a drop. Axisymmetry is not broken, and Matlab can succesfully use the polynomial fitting function `polyfit` to fit the curve to a 2nd-order polynomial.

4 Instructions - Walk through all steps

In this section we walk through the steps needed to align the tensiometer, take a series of images, make measurements on the images, and describe what the output means. Refer to Figure 3 as a graphical aid.

4.1 Setting up

Align setup - You want as much of the camera's CCD lit as uniformly as possible with the magnification such that all of the drop fits into the CCD. For the current method of edge extraction, the rows containing

the drop should be completely bare except for those pixels within the confines of the drop. To avoid image processing, the illumination circle should be kept larger than the image.

1. Run a program to stream video from the camera's CCD. The system described here uses a small LabVIEW script called "Grab Example.vi" from Scion. Use this feed to finetune the focus and magnification. Adjust the focus to the object plain using the objective lens.

2. Once the video feed, or another way of confirming the optics is ready, we need to set up Koehler illumination to get uniform lighting conditions and sharp focus.[2]

   (a) First, check that the edges of the field diaphragm are sharply imaged onto the video feed by almost completely closing the field diaphragm. If you do not see the crisp edges of the diaphragm, you may need to slide the field diaphragm along the rail until it is imaged on the object plane. A quick method to confirm that the field diagram is in the correct spot is to shine a light of the same wavelength as the light source from the object plane through the lens and onto the closed aperture stop. If the light is in focus on the field diaphragm, then it is in the right spot.

   (b) Now that the Field diaphragm is confirmed, check the position of the aperture diaphragm by seeing if the light source is imaged sharply on the aperture diaphragm. Open the field diaphragm and close the aperture diaphragm. Observe that the light source is visible in sharp focuson the aperture diaphragm. If not, slide it along its rail until it is.

We are done setting up illumination and need to make sure that our image is in focus. Fill cuvette with fluid and place it in the index matching container. Be aware that the cuvette is prone to floating away, and must be carefully placed in the index matching container so as to not tip over of float away.

1. We can confirm that the focus is on the object plane through a quick test: slide the needle low enough so that, on the video feed, it looks like a thick vertical line cutting through the whole image. If the image of the needle is pinched in the middle, or its edges are not sharp, you need to adjust focus by sliding the objective. Stop when that needle has uniform width at each point on the image. Keep in mind that the needle is only being used as a marker to help with setting up focus and another marker is probably just as suitable.

2. Get focus for the desired magnification by shifting the objective or camera one at a time. Remember the quick relation Magnification $= \frac{\text{object-objective distance}}{\text{object-camera distance}}$. Make sure that the image isn't warped, pinched, or out of focus.

In order to manuever the syringe tip, slide the syringe controller (Figure 3B,C) down the vertical rail to which the XYZ stage is attached to by a dolly until the tip of the syringe is near the desired level. Now, using the three knobs on the XYZ stage, finetune the position of the tip, until it is in focus, in the desired place on the video feed.

[2] If necessary, refer to section 2.1.1 for tips on creating Koehler illumination.

4.2 Running the experiments (taking images)

The setup is now tuned. Make sure your syringe is filled with the desired fluid, and maneuver the syringe so that its tip is visible at the top center of the image on the CCD (or bottom in the case of an inverted system). The width of the tip will be the known feature used to extract converting the drop from pixels to meters, so make sure it is visible.

- Turn off video streaming, and prepare the camera to take a time sequence of images. The system described here uses a small LabVIEW script called "Snap Sequence.vi" developed in house. There is nothing noteable about the script except that it takes a user-specified number of images at a constant, user-specified time interval. Each image is saved sequentially with a name corresponding to its image index, starting from "0001". There is an absolute maximum of 9,999 images because the naming scheme for the saved images only supports image names "0001" through "9999". The images need to be saved as .jpg files.

- Once the camera is ready, run the Snap Sequence program. Choose or create a folder with a descriptive name for the experiment. Make sure to record $\Delta\rho$ and the gauge of the syringe tip somewhere (possibly in the folder name). For the duration of the experiment, use the micrometer to help smoothly dispense fluid from the syringe. Dispense fluid in a manner according to your experiment. Stop either at the end of the image sequence, or when the syringe is empty or when the micrometer has extended to its full length. If the micrometer extends to its maximum length partway through the experiment, spin it backwards to detract the head completely and slide the micrometer holder down along its rail so that the micrometer tip is resting on the syringe plunger again. If vibrations are an issue, remove the micrometer and its holder from the rail before detracting it and re-attach it to the rail afterwards.

- The images may require some processing to be accepted by the current edge-extraction algorithm. If the illumination circle is small enough that its edge can be seen on the sides of the image, then the image either needs to be cropped or the area outside the illumination circle needs to filled to the color of the background. See section 3.1.4 for more details about the edge-extraction algorithm to decide on the best approach suited for your optical reality.

4.3 Making measurements

1. Open the GUI using matlab's guide tool to avoid complications. If guide is unavailable, feel free to open the GUI's .fig file but it may not respond to input. If you see an error in the Command Window saying "Attempt to reference field of non-structure array", close the GUI and open it through guide. If you want to edit the GUI, make sure you do it through guide unless you know what you are doing. The reason for this is the GUI is written using Matlab's Graphical User Interface Development Environment (guide). As a result, the GUI is not as robust as it should be. It is suggested that the GUI be opened from within guide. Guide can be opened by typing `guide` on the command line.

2. If you want to use estimation to automatically find initial parameters, proceed to step 4.

3. When the GUI initially opens, a default table of S vs. H^{-1} is loaded. However, if you turn off estimation by depressing the ESTIMATE MODE you will be able to supply initial parameters manually by filling in INITIAL B and INITIAL A. Toggling ESTIMATE MODE on again, prompts the user to choose the file holding a table of S vs. H^{-1} values.

4. Choose the image folder by clicking SELECT IMAGE FOLDER.. This selects the directory containing the sequence of drops to analyze. The filepath is displayed.

5. Set the NUMBER OF ROTATIONS to specify the number of 90° ccw rotations to apply to the image.

6. Once you have chosen an image folder, the "0001.jpg" image from that folder will be put through the imaging algorithm described in Section 3.1.3. Specifically it will be rotated and displayed in grayscale. Use this image to determine the starting row and confirm that you have the right number of rotations.

7. The STARTING ROW (Y) is the topmost row of the image for which at least one side of the drop connects to the needle. It is the row of the basis.[3] If images of the drops had no tilt, then the starting row would be the row at which the drop connects to the needle; however, in images where a drop is tilted, it is necessary to select the topmost row where a drop is in contact with the needle. We use the value of the starting row in the edge extraction algorithm described in section 3.1.4.

8. Now you need to set the scaling factor, which is the ratio of the SCALING FACTOR (M) and SCALING FACTOR (PX). As long as their ratio is maintained, the actual values of the scaling factor input doesn't matter; however, it is a good idea to use the outer diameter of the needle for the two inputs: SCALING FACTOR (PX) can be the outer diameter of the needle in pixels and SCALING FACTOR (M) can be the outer diameter of the needle in m. The scaling factor is used to scale the extracted drop from pixel units to meters. This is necessary because the Young-Laplace equations in this implementation are in units of meters.

9. Put in the DEL RHO IN (KG/M^3), the density difference in kilograms per cubic meter of the two materials. This value is technically the absolute value of the density difference.

10. VIEW SELECTED DROP can be used after an image folder is selected and the user has selected a drop. A drop is selected by either double clicking on an image file name from the list or writing its filepath directly in the text field to the right of the SELECT IMAGE FOLDER.. button.

11. Choose one of DIRECTORY MODE, or SELECTED DROP to specify whether the whole directory or just one image is displayed. If directory mode is selected, all the images in the folder are measured and saved as an array of inputs and outputs and estimates (see Section 4.4 for contents of Input and Output). Additionaly, the GUI window is closed if the whole directory is imaged. If selected drop mode is chosen, only the selected drop selected in the files list is measured and its inputs and outputs and estimates are saved. Additionally, an image of both the experimental and theoretical curve is plotted. See step 10 for instructions on selecting a drop.

12. The file holding the inputs, outputs, and estimates as cells (see Section 4.4 for contents of each cell) will be saved to a file called drop_profile_mm_dd_yy_HHMM, where mm, dd, yy, HH, MM is the numerical month, day, year, hour, and minute, respectively, of the time right before the file begins to save to disk.

[3] Note that in Matlab, the default setting is to display an image with the origin at the top-left of the screen. When describing images we assume that they have already been rotated so that the base of the drop is towards the bottom of the screen and the apex of the drop is towards the top.

4.4 Reading measurements

This is a list of inputs and outputs with a brief summary to be used for reference when looking at measurements saved by the current version of . Note that this section may be out of date in further revisions of implementation.

- INPUT:
  - start_row - The bottom-most row of the image where to search for the drop. (i.e. row just above tip of the needle)
  - thresh - Threshold pixel value at which to detect the drop (0 is dark, 256 is white). Anything lower than this value represents a drop.
  - filepath - the complete path to a file holding the image. Should be of type .jpg
  - num_rotations - The number of 90 degree counter clockwise rotations to apply to the image in filepath
  - init_bguess - Initial Guess for shape parameter (radius of curvature) b
  - init_aguess - Initial Guess for capillary constant a
  - conv - Conversion Factor:
    $conv = (\Delta\rho \text{ in kg/m}^3) * (g \text{ in m/s}^2)$ in units of $(\text{kg/m}^3)(\text{m/s}^2) = \text{kg} * \text{s}^{-2} * \text{m}^{-2}$
  - scale - Scaling factor = (Needle Width in m)/(Needle Width in Pixels). Used to scale drop edge from pixel units to meters.
- OUTPUT:
  - curv - curvature in inverse meters = (shape parameter $b)^{-1}$
  - cap - capillary constant in meters a
  - bond - cap*(curv^2)
  - gamma - Gamma in Newtons/meter
  - area - Calculated Area in meters^2 from theoretical curve
  - vol - Calculated Volume in meters^3 from theoretical curve
  - Am - Measured Area in meters^2 from extracted edge
  - Vm - Measured Volume in meters^3 from extracted edge
  - gamma_unc - gamma uncertainty from fitting
  - cap_unc - capillary constant uncertainty from fitting
  - area_err - Area error fraction = $((Area_{experimental}) - (Area_{theoretical}))/(Area_{experimental})$
- ESTIMATES:
  - gamma_estimate - estimated value of γ
  - b_estimate - estimated value of b
  - a_estimate - estimated value of a
  - S - ratio of equatorial diameter to selected plane diameter

5 Resulting Values for real drops

Work is under way characterizing the accuracy of the tensiometer. Preliminary results on critical drops suggest that the tensiometer can accurately predict drop shapes to within 2%. A set of water drops were simulated by integrating the Young Laplace equations with b varying from 0.00136275 to 0.00210525 meters. The current implementation of the tensiometer only allows critical drops to be measured or simulated.

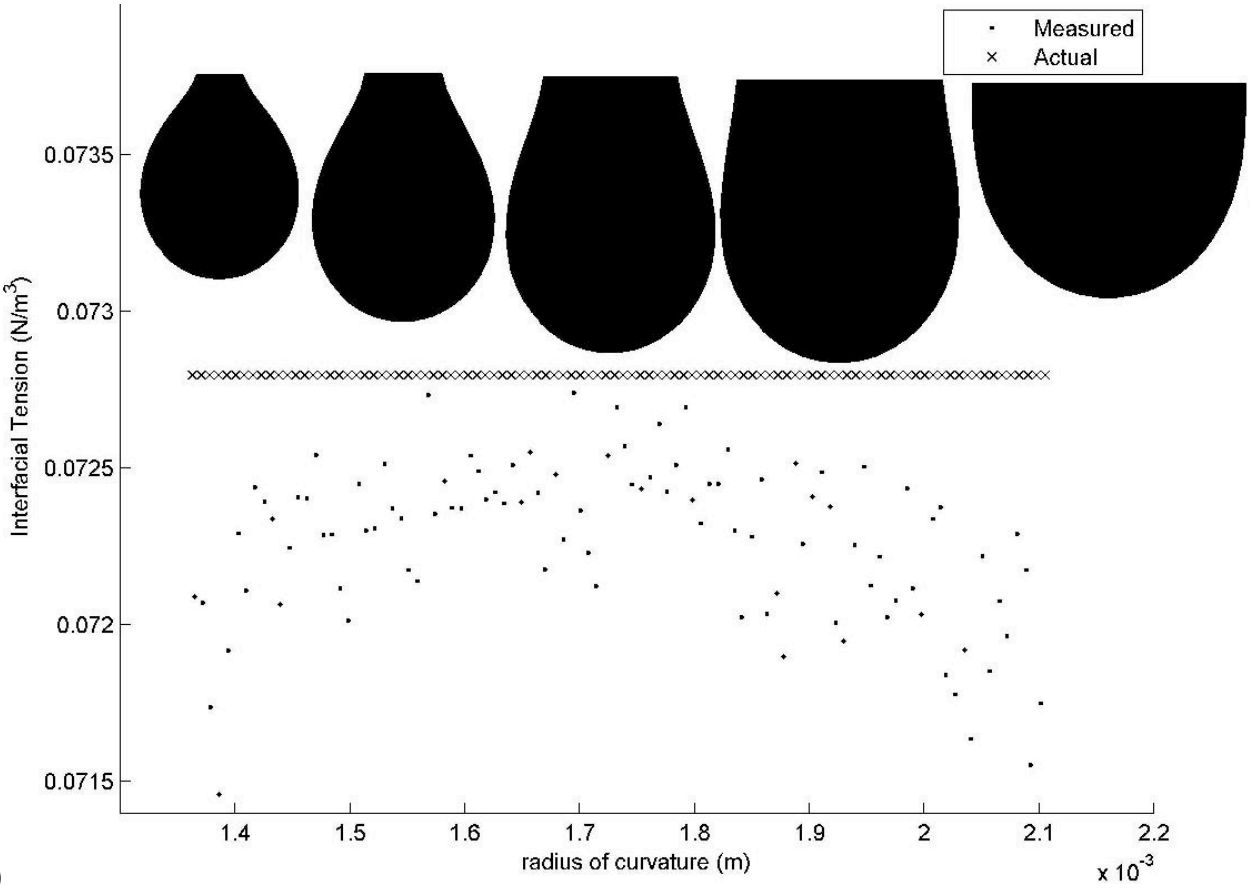

(A)

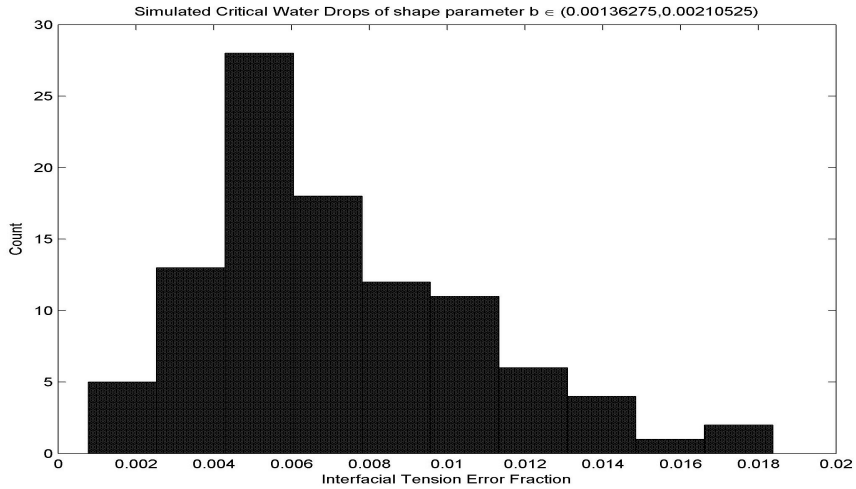

(B)

Figure 5: A set of simulated critical water drops of varying radius of curvature from 0.00136275 to 0.00210525 meters. (A) Radius of curvature in meters for inset drops from left to right: 0.001362750, 0.001542750, 0.001730250, 0.001917750, 0.002105250 (B) Histogram of γ measurement error w.r.t. actual γ. All 100 drops have less than 2 percent error.

Contents

1 Theory **2**
1.1 Interfacial Tension . . . 2
1.2 Young-Laplace Equations . . . 3
1.3 Estimation methods . . . 6
1.3.1 Selected Plane Method: . . . 6
1.3.2 Oscullating circle . . . 7

2 Setup **9**
2.1 Optics . . . 9
2.1.1 Koehler Illumination . . . 9
2.1.2 Index Matching the Cuvette . . . 10
2.2 Syringe Controller . . . 11

3 Software **13**
3.1 Tensiometer Software . . . 13
3.1.1 GUI . . . 13
3.1.2 Imaging . . . 14
3.1.3 Edge Extraction Algorithm . . . 14
3.1.4 Estimating Parameters . . . 15

4 Instructions - Walk through all steps **15**
4.1 Setting up . . . 15
4.2 Running the experiments (taking images) . . . 17
4.3 Making measurements . . . 17
4.4 Reading measurements . . . 19

5 Resulting Values for real drops **20**

References

[1] JM Andreas, EA Hauser, and WB Tucker, The Journal Of Physical Chemistry 42, 1001. 1019 (1938).

[2] T.Y. Latychevskaia and E.C. Meister, Journal Of Chemical Education 83, 117 (2006).

[3] B Song and J. Springer, Journal Of Colloid And Interface Science 184, 64-76 (1996).

[4] A Gray, "Osculating Circles to Plane Curves." §5.6 in Modern Differential Geometry of Curves and Surfaces with Mathematica, 2nd ed. Boca Raton, FL: CRC Press, pp. 111-115, 1997.

[5] Z Pardey, Thesis, Brandeis University (2009).

[6] Claeys, J. http://home.scarlet.be/~ping1339/curves.htm#Osculating-circle (1997)